INL/EXT-16-40046 Rev. 0

September 2016

High-Burnup-Structure (HBS): Model Development in MARMOT for HBS Formation and Stability Under Radiation and High Temperature

K. Ahmed
X. Bai
Y. Zhang
B. Biner

INL/EXT-16-40046 Rev. 1

High-Burnup-Structure (HBS): Model Development in MARMOT for HBS Formation and Stability Under Radiation and High Temperature

K. Ahmed
X. Bai[*]
Y. Zhang
B. Biner

September 2016

Idaho National Laboratory
Fuel Modeling and Simulation Department
Idaho Falls, Idaho 83415

[*]**Virginia Polytechnique Instuitute and State University**
Department of Materials Science and Engineering
Blacksburg, VA

Prepared for the
U.S. Department of Energy
Office of Nuclear Energy
Under U.S. Department of Energy-Idaho Operations Office
Contract DE-AC07-99ID13727

ABSTRACT

A detailed phase field model for the formation of High Burnup Structure (HBS) was developed and implemented in MARMOT. The model treats the HBS formation as an irradiation-induced recrystallization. The model takes into consideration the effect of the stored energy associated with dislocations formed under irradiation. The accumulation of radiation damage, hence, increases the system free energy and triggers recrystallization. The increase in the free energy due to the formation of new grain boundaries is offset by the reduction in the free energy by creating dislocation-free grains at the expense of the deformed grains. The model was first used to study the growth of recrystallized flat and circular grains. The model reults were shown to agree well with theoretical predictions. The case of HBS formation in UO_2 was then investigated. It was found that a threshold dislocation density of $3.3-5\times10^{14}\,\mathrm{m}^{-2}$ (or equivalently a threshold burn-up of 33-40 GWd/t) is required for HBS formation at 1200K, which is in good agreement with theory and experiments. In future studies, the presence of gas bubbles and their effect on the formation and evolution of HBS will be considered.

Table of Contents

1. Introduction

UO_2 and other nuclear fuels develop a unique microstructure under irradiation usually known as the High Burn-up Structure (HBS) [1-5]. In this HBS, the as-fabricated microstructure transforms into a much finer one with a grain size that is orders of magnitude less than the initial grain size. The reduction of the strain energy, due to point defects and dislocations formed during irradiation-by forming new defect, free subgrains offsets the excess energy required for creating new grain boundaries. The HBS is also a very porous structure, where gas bubbles usually decorate the grain boundaries of the fine, newly formed subgrains. It was shown that the HBS formation alters the mechanical and thermal properties of nuclear fuels [1-5]. It also changes the swelling and gas release rates and hence affects the fuel integrity and performance. Therefore, investigating the formation and evolution of the HBS in nuclear fuels is of paramount importance for improving the reactor performance and safety.

Two main mechanisms for the HBS formation were proposed in literature, e.g., polygonization and recrystallization [1-5]. Polygonization is the subdivision of the original grains based on the reorganization of dislocations into sub-boundary domains. Recrystallization is characterized by the formation of subgrains and their subsequent growth into stable recrystallized grains. We focus here on the latter mechanism.

A quantitative phase field model of irradiation-induced recrystallization was developed and implemented in MARMOT. The model adds the stored energy contribution, associated with dislocations formed under irradiation, to the regular grain growth model [6, 7] to account for the formation and subsequent growth of recrystallized grains. Stored energy kernel, action and material class were added to MARMOT to facilitate the implementation of the model. The model

predicts a threshold dislocation density of $3.3-5\times10^{14}\,\mathrm{m}^{-2}$ (or equivalently a threshold burn-up of 33-40 GWd/t) for the formation of HBS in UO_2 at 1200K, which agrees well with theoretical predictions and experiments [1-5]. The formation of gas bubbles and their effect on the formation and evolution of the HBS will be investigated in future studies.

2. Phase field modeling of irradiation-induced recrystallization

The model utilized here is based on the model by Moelans et. al. for investigating the migration of recrystallization boundaries [8]. However, we account here for the accumulation of radiation damage in grains by incorporating a dislocation density field. The model can be summarized as follows. A set of non-conserved order parameters (phase fields) is used to represent different grains with different orientations as in the regular grain growth models [6-8]. Each grain is assigned a dislocation density ρ_i and the average/effective dislocation density ρ_{eff} in the system is calculated as,

$$\rho_{\mathrm{eff}} = \frac{\sum_i \rho_i \eta_i^2}{\sum_i \eta_i^2}. \tag{1}$$

here, p is the total number of order parameters. The deformation/stored energy associated with this dislocation density is then given by

$$g(\rho_{\mathrm{eff}},\eta_1,...,\eta_p) = \frac{1}{2}\mu b^2 \rho_{\mathrm{eff}}, \tag{2}$$

where μ is the shear modulus and b is the length of the Burgers vector.

The total free energy of the system can be constructed as follows [8]

$$F = \int f(\eta_1,...,\eta_p) + g(\rho_{\mathrm{eff}},\eta_1,...,\eta_p) + \frac{1}{2}\sum_{\alpha=1}^{p} \kappa_\eta \left|\nabla \eta_\alpha\right|^2 \quad d^3r, \tag{3}$$

where, besides the stored/deformation energy term the other two terms are the same as in grain growth models. Specifically, we use

$$f(\eta_1,...,\eta_p) = A[0.25 + 0.25\sum_i \eta_i^4 - 0.5\sum_i \eta_i^2 + 1.5\sum_i \sum_j \eta_j^2 \eta_i^2]. \quad (4)$$

A and κ_η are material constants related to grain boundary energy and thickness.

The non-conserved order parameters evolve according to Allen-Cahn equations [6-8] as

$$\frac{\partial \eta_\alpha}{\partial t} = -L\left[\frac{\partial f(\eta_1,....,\eta_\alpha,....,\eta_p)}{\partial \eta_\alpha} + \frac{\partial g(\rho_{\text{eff}},\eta_1,....,\eta_\alpha,....,\eta_p)}{\partial \eta_\alpha} - \kappa_\eta \nabla^2 \eta_\alpha\right] \quad \forall \alpha, \alpha = 1, 2....p\,. \quad (5)$$

Here, L, the Allen-Cahn mobility, is a material property that is related to the grain boundary mobility [6-8]. Using constant gradient and mobility coefficients is equivalent to the assumption of isotropic grain boundary energy and mobility.

The effective dislocation density is prescribed according to a constitutive law. We simply use here an empirical relation that calculates the average dislocation density for a given burn-up (Bu), e.g., [5]

$$\log \rho_{\text{eff}} = 2.2 \times 10^{-2}\,\text{Bu} + 13.8\,. \quad (6)$$

The deformed grains are assumed to have this dislocation density, while the recrystallized grains are dislocation-free.

In order to implement this model in MARMOT, a kernel that accounts for the stored energy associated with dislocations has been created. Moreover, an action (called Polycrystal Stored Energy) to add this stored energy for each order parameter/grain was also constructed. A Material calass (called Deformed Grain) was also used to specify the dislocation density and model parameters for simulations.

The phase field model parameters are directly related to the thermodynamic and kinetic parameters as follows [6-8]

$$A = \frac{3\gamma_{\mathrm{b}}}{4\ell}, \tag{7a}$$

$$\kappa_{\eta} = \frac{3}{4}\gamma_{\mathrm{b}}\,\ell, \tag{7b}$$

$$L = \frac{4M_b}{3\ell}\ . \tag{7c}$$

In the above, ℓ is the diffuse interface width, γ_{b} is the grain boundary energy, and M_{b} is the grain boundary mobility. The grain boundary energy of UO_2 is taken to be 1.58 J/m^2 [9]. The grain boundary mobility of UO_2 is given by [10]

$$M_{\mathrm{b}} = 9.21\times10^{-9}\exp(-2.77\mathrm{eV}/k_B T)\ \ \mathrm{m}^4/\mathrm{J.s.} \tag{8}$$

The shear modulus and the magnitude of the Burgers vector for UO_2 are taken as [4] $\mu = 2\times10^{11}\mathrm{J/m}^3$, $b = 0.547\mathrm{nm}$. A temperature of 1200K is assumed for all the simulations conducted here.

3. Results and discussion

We have carried out several 2D simulations for investigating the irradiation-induced recrystallization. We present and discuss the results of these simulations in this section. First, we study the growth rate of a recrystallized grain and compare it with theoretical predictions. We then investigate the irradiation-induced recrystallization (formation of the HBS).

3.1 The growth rate of a recrystallized grain

Before investigating the nucleation/recrystallization of grains, we study the growth of a recrystallized grain. This test case is studied first since it provides a benchmark for the model.

The velocity (v) of the grain boundary of a recrystallized grain growing at the expense of a deformed grain is given by

$$v = M_{\mathrm{b}}(g - \gamma_{\mathrm{b}}\kappa) = \frac{3L\ell}{4}(g - \gamma_{\mathrm{b}}\kappa)\,. \tag{9}$$

In the above, g is the stored energy given by Eq. (2) and κ is the grain curvature. In the second equality we used the relation of Eq. (7c) to express the grain boundary velocity in terms of the phase field model parameters.

We first study the growth of a recrystallized flat grain. The domain size was $1.28\mu\mathrm{m} \times 1.28\mu\mathrm{m}$. The thickness of both the recrystallized and deformed grain was $0.64\mu\mathrm{m}$. The interface width was taken to be 40 nm. The deformed grain was assumed to have a dislocation density, $\rho_{\mathrm{eff}} = 1 \times 10^{-15}\mathrm{m}^{-2}$, while the recrystallized grain is dislocation-free. Snapshots of the evolution of the recrystallized grain are shown in Fig. 1. Evolution proceeds until the deformed grain completely disappears. In this case, the grain boundary velocity is simply given by, $v = M_{\mathrm{b}}\, g = 3L\ell g / 4$. Since the velocity of the flat grain can expressed in terms of its thickness as dx / dt , the thickness of the recrystallized flat grain increases with time as

$$x - x_0 = k\,t\,, \tag{10.a}$$

$$k = M_{\mathrm{b}}\, g = 3L\ell g / 4\,. \tag{10.b}$$

The increase of the recrystallized flat grain is captured in Fig. 2. The rate constant (k) calculated from the simulation was $k = 2.49 \times 10^{-4}$, which is very close to the exact value $k = 2.57 \times 10^{-4}$ expected from Eq. (10).

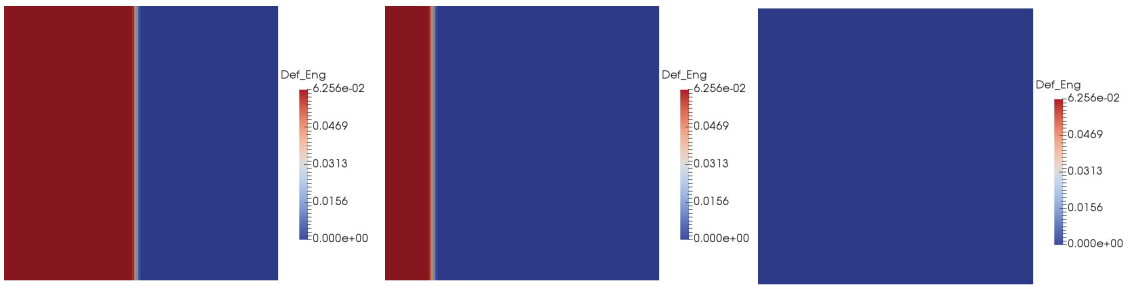

Fig. 1. Snapshots of the growth of a recrystallized (dislocation-free) flat grain at the expense of a deformed flat grain. The deformed grain has a dislocation density, $\rho_{\text{eff}} = 1\times10^{-15}\,\text{m}^{-2}$. The stored/deformation energy shown in the figure (Def_Eng) is in eV/nm^3.

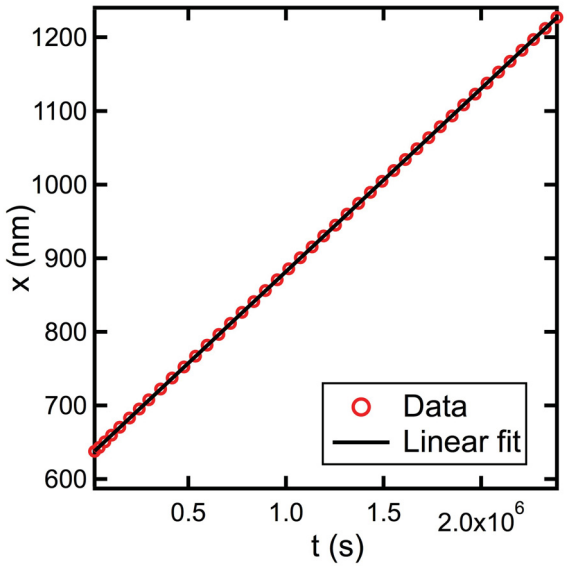

Fig. 2. The increase in the thickness of the recrystallized slab grain shown in Fig. 1. The growth follows the linear relation predicted by Eq. (10).

We then investigate the growth/shrinkage of a recrystallized circular grain embedded in a deformed matrix grain. According to Eq. (9), the velocity of a circular grain reduces to

$$v = M_{\text{b}}(g - \frac{\gamma_{\text{b}}}{R}) = \frac{3L\ell}{4}(g - \frac{\gamma_{\text{b}}}{R}), \tag{11}$$

where, is the grain radius. In contrast to the case of a flat grain, a circular grain may grow or shrink depending on the value of its radius and the dislocation density (and hence the stored energy) in the deformed grain. For a given dislocation density, a critical radius can be defined

where a grain with a larger radius grows and a grain with a smaller radius shrinks. From Eq. (11), and considering Eq. (2), the critical radius is given by

$$R^{\mathrm{c}} = \frac{\gamma_{\mathrm{b}}}{g} = \frac{2\gamma_{\mathrm{b}}}{\mu b^2 \rho_{\mathrm{eff}}}. \tag{12}$$

Of course, one can instead define a critical dislocation density for the deformed grain for a particular initial radius of the recrystallized grain. In this case, the recrystallized grain will grow only if the dislocation density in the deformed grain is higher than the critical value, e.g., .

$$\rho_{\mathrm{eff}}^{\mathrm{c}} = \frac{2\gamma_{\mathrm{b}}}{\mu b^2 R}. \tag{13}$$

We conducted a few 2D simulations in order to explore these different scenarios using our phase field model. The domain size was $1.28\mu\mathrm{m} \times 1.28\mu\mathrm{m}$. The interface width was taken to be 40 nm. Periodic boundary conditions were applied in both directions. The initial grain radius of the recrystallized grain was 160 nm. From Eq. (13), the critical dislocation density that corresponds to that radius is $\rho_{\mathrm{eff}}^{\mathrm{c}} = 3.3 \times 10^{14}\mathrm{m}^{-2}$. We carried out three different simulations with three values for the dislocation density in the deformed grain, e.g., $\rho_1 = 2.3 \times 10^{14}\mathrm{m}^{-2}$, $\rho_2 = 3.3 \times 10^{14}\mathrm{m}^{-2}$, and $\rho_3 = 4.3 \times 10^{14}\mathrm{m}^{-2}$. In agreement with the predictions of Eqs. (11-13), the recrystallized grain grew when the dislocation density was higher than the critical value and shrank when it was lower. The grain radius stayed constant when the dislocation density was equal to the critical value. These results are demonstrated in Fig. 2. and Fig.3. below. Fig. 2. captures the growth/shrinkage of the recrystallized grain at the expense of the deformed matrix grain. The change of the recrystallized grain radius with time for different dislocation densities is depicted in Fig. 3.

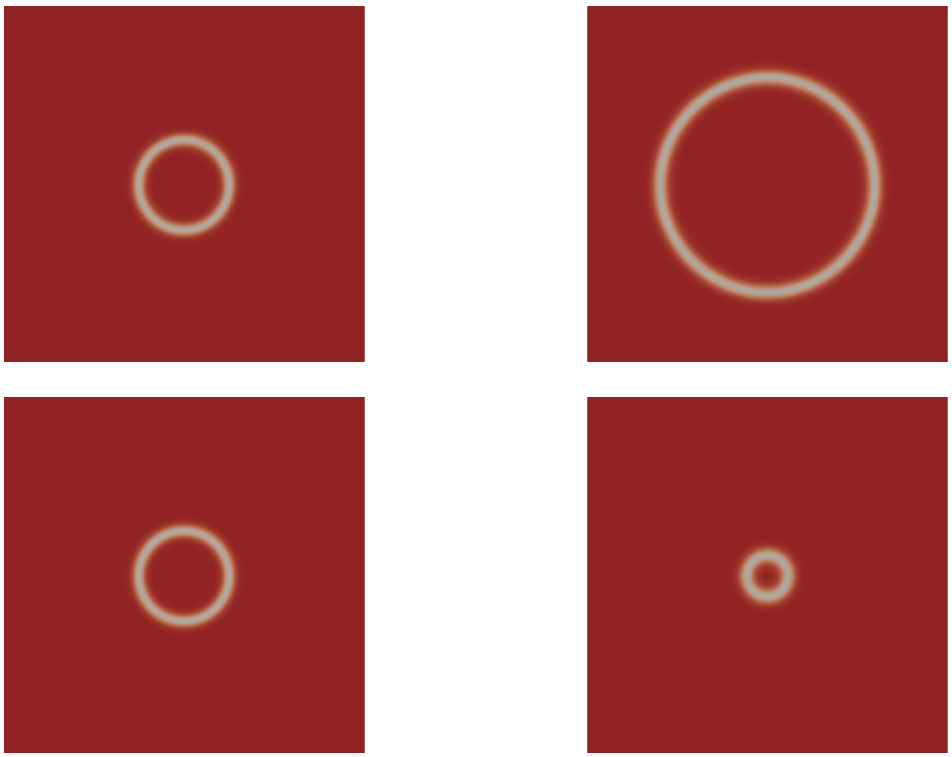

Fig. 3. Snapshots of the growth (upper row)/shrinkage (lower row) of a recrystallized circular grain embedded in a deformed matrix grain. When the dislocation density in the deformed grain is higher than the critical value (see Eq. (13)), the recrystallized grain grows; while it shrinks if the dislocation density in the deformed grain is lower than the critical value.

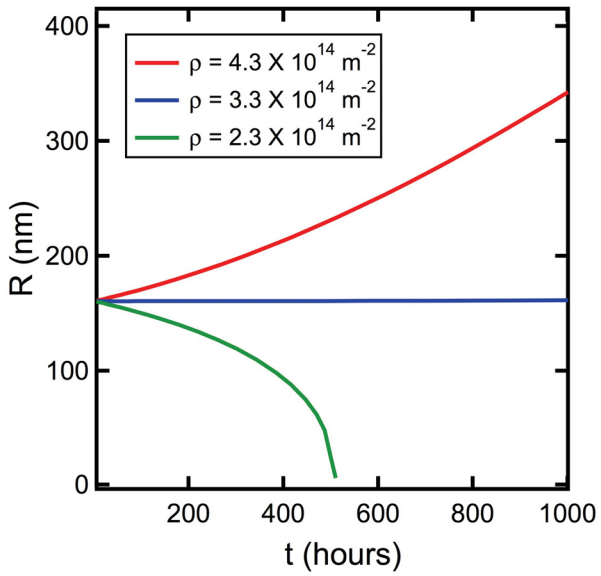

Fig. 4. The evolution of the radius of a recrystallized circular grain embedded in a deformed matrix grain for different values of the dislocation density (see Fig. 3). The grain radius increases when the dislocation density is higher that the critical value ($\rho_{\text{eff}}^{\text{c}} = 3.3\times10^{14}\,\text{m}^{-2}$) and decreases if the dislocation density in the deformed grain is lower than the critical value. The grain radius stays constant when the dislocation density takes on its critical value.

3.2 Simulations of HBS formation

We present here 2D simulations of irradiation-induced recrystallization. In phase field models, two different methods are usually used to induce nucleations [11]. The classical and most rigorous way is to directly include Langevin type fluctuations in the evolution equations. The other method is basically to directly introduce new stable nuclei with a specific rate that can be estimated from the classical nucleation theory. Each method has its own advantages and drawbacks. We choose here a simpler version of the first method where fluctuations are only considered in the initial conditions. We use an extra set of order parameters that initially do not represent any grains, but can represent any new grains that may form. These order parameters are randomly initialized with values less than 10^{-3}. The aaditional extra order parameters evolve via the same evolution equation as the regular order parameter set that represent the initially

deformed grains. This increase in the computational time due to the extra set of order parameters can be reduced using the Grain Tracker algorithm already implemented in MARMOT [7]. This algorithm can be used to represent a large number of grains using a small set of order parameters. We used it here to handle both types of grains, e.g., the initially deformed ones and the recrystallizing ones. All the kernel and material classes were constructed to be compatible with such implementation.

We first studied the case of irradiation-induced recrystallization at the boundary of a deformed bicrystal. The domain size was $12.8\mu\text{m} \times 12.8\mu\text{m}$. The thickness of both of the initially deformed grains was $6.4\mu\text{m}$. The interface width was taken to be 400 nm. Natural boundary conditions are used. Two order parameters represent the two deformed grains and extra set of four order parameters were reserved for nucleation of new grains. Different dislocation densities were considered to study the effect of the dislocation density on the recrystallization process. As we discussed before, there is a critical dislocation density for a recrystallized grain to grow. Therefore, one would expect the same for nucleation since if the nuclei cannot grow into stable size grains they will eventually disappear. Indeed, our simulations demonstrated that a threshold dislocation density $\rho_{\text{eff}}^{\text{c}} = 3.3 \times 10^{14}\,\text{m}^{-2}$ is required for recrystallization to take place. This is captured in Figs. 5 and 6. Fig 6 shows snapshots of the recrystallization process for two different dislocation densities higher than the threshold value. The higher the dislocation density is, the larger the number of recrystallized grains is. This is consistent with the fact that there is an energy cost associated with the formation of a grain boundary. The recrystallized grains grow at the expense of the initially deformed bicrystal until they consume the whole domain. The fraction of the recrystallized grains as function of time is captured in Fig. 6. As evident from the figure, no recrystallization takes place unless the dislocation density is higher than the threshold

value. Moreover, as the dislocation density increases, the incubation time (the time before the first nucleation event) decreases.

Lastly, we present some preliminary results for irradiation-induced recrystallization in polycrystalline UO_2. The domain size was $2.56\mu\text{m} \times 2.56\mu\text{m}$. The interface width was taken to be 40 nm. Periodic boundary conditions were used. The domain initially had 30 deformed grains. An extra set of 10 order parameters were reserved for the nucleation of new grains. The average dislocation density was $\rho_{\text{eff}} = 6 \times 10^{14}\,\text{m}^{-2}$, which is equivalent to a burn-up of 45 GWd/t. The evolution of the microstructure during recrystallization is depicted in Fig. 7. The recrystallized grains first appear at triple- and higher-order junctions and continue to grow at the expense of deformed grains. The number of grains was doubled by the end of the simulation. Larger domains with larger number of grains will be considered in future studies.

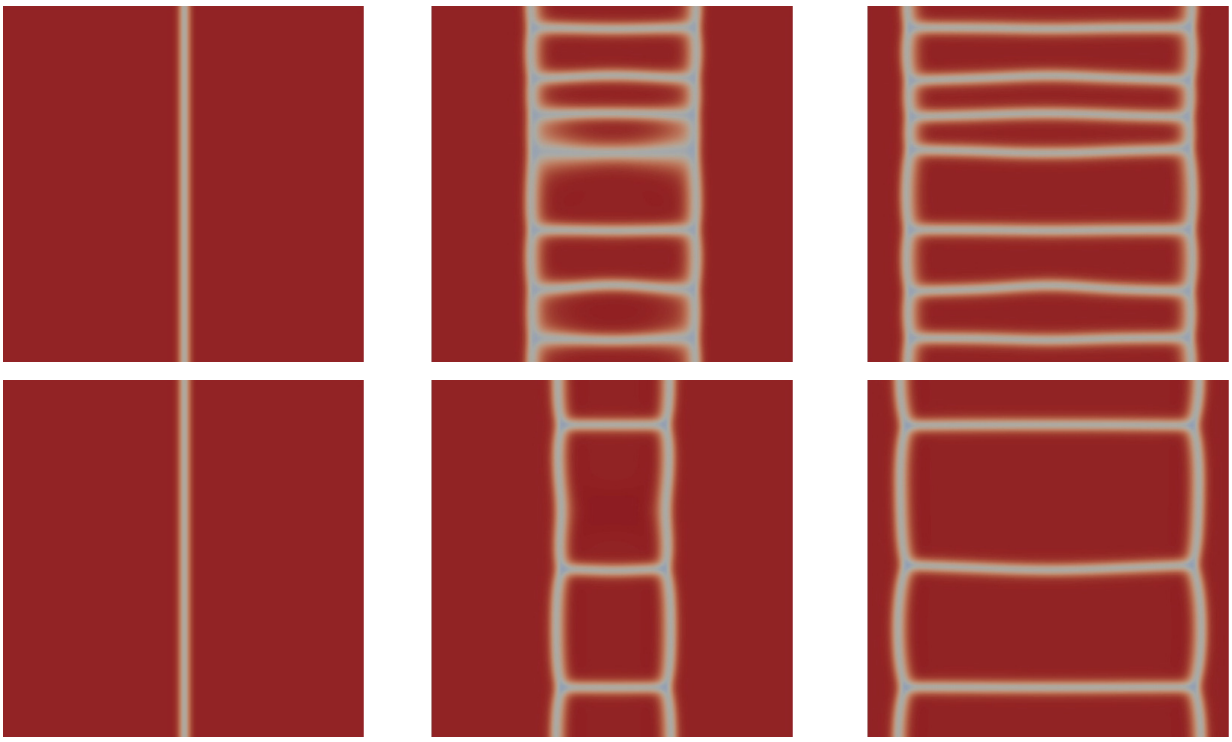

Fig. 5. Snapshots of the irradiation-induced recrystallization for an initially deformed UO_2 bicrystal with $\rho_{\text{eff}} = 6.6\times10^{14}\,\text{m}^{-2}$ (upper row) and $\rho_{\text{eff}} = 3.3\times10^{14}\,\text{m}^{-2}$ (lower row) at 1200K. More recrystallized grains are formed as the dislocation density increases.

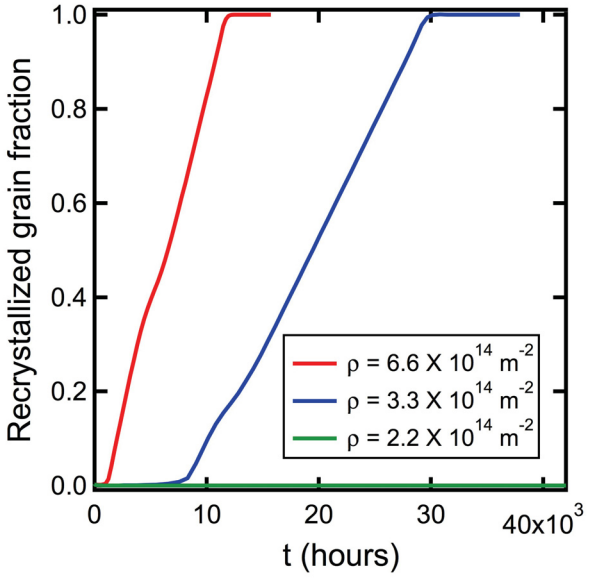

Fig. 6. The area fraction of the recrystallized grains shown in Fig. 5. Recrystallization proceeds only if the dislocation density is higher than a threshold value. The higher the dislocation density is, the shorter the incubation period is.

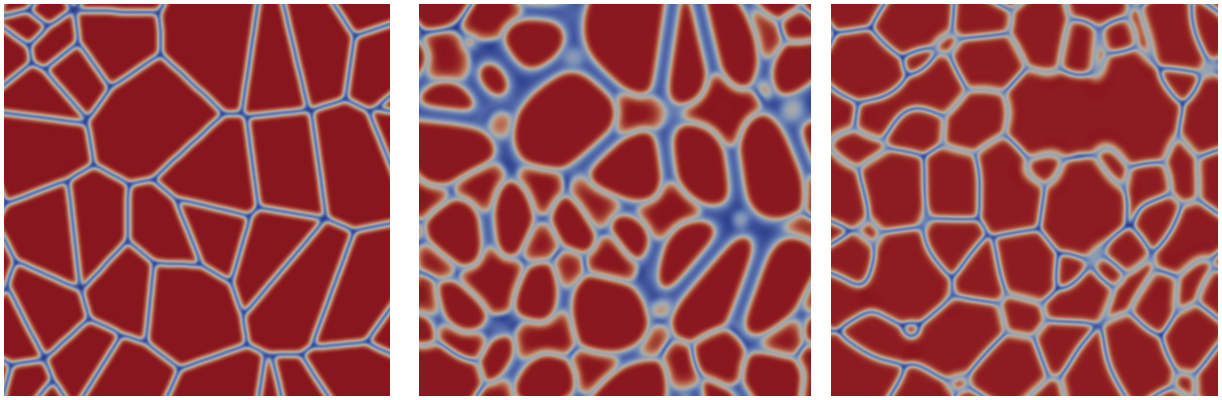

Fig. 7. Snapshots of irradiation-induced recrystallization in polycrystalline UO_2 at 1700K. The recrystallized grains first appear at triple- and higher order-junctions and then grow at the expense of the original deformed grains. The increase of number of grains and hence reduction in the average grain size is evident.

4. Summary

A novel quantitative phase field model for irradiation-induced recrystallization was introduced and implemented in MARMOT. The model accounts for the stored energy associated with dislocations created during irradiation. Recrystallization takes place by creating new dislocation-free subgrains that grow into stable grains. The reduction in the free energy by forming dislocation-free grains at the expense of deformed grains offsets the increase in the free energy due to the creation of new grain boundaries. The model was benchmarked against analytical results of the growth of recrystallized flat and circular grains. The model predicts a threshold dislocation density for the HBS formation in agreement with theory and experiments. For polycrystalline UO_2 at 1200K, the recrystallized average grain size was found to be on the order of 100 nm at a threshold dislocation density of $3.3-5\times10^{14}\,\mathrm{m}^{-2}$ (or equivalently a threshold burn-up of 33-40 GWd/t), which agrees well with experiments [1-5].

While the model has been implemented in MARMOT in a way compatible with Grain Tracker [7] to reduce the computational cost, some issues arise during the simulation of recrystallization with large number of grains. These issues occur when multiple nucleation events of new grains take place at the same time. In such situation, Grain Tracker faces diffculity in re-mapping the grains with the same order parameter away from each other to prevent unphysical merging. We will modify the nucleation method and or Grain Tracker to alleviate this problem. Furthermore, to fully describe the HBS formation and evolution, the presence of gas bubbles and their interactions with the recrystallized grains must be included in the model. This will be the subject of a future investigation.

References

[1] J. Rest and G. Hofman, Journal of Nuclear Materials **210**, 187-202 (1994).
[2] J. Rest, Journal of Nuclear Materials **346** (2–3), 226-232 (2005).
[3] J. Rest, Journal of Nuclear Materials **349** (1-2), 150-159 (2006).
[4] H. Xiao, C. Long and H. Chen, Journal of Nuclear Materials **471**, 74-79 (2016).
[5] K. Nogita and K. Une, Journal of Nuclear Materials **226**, 302-310 (1995).
[6] N. Moelans, B. Blanpain, and P. Wollants, Physical Review B **78**, 024113 (2008)
[7] C. Permann, M. Tonks, B Fromm, and D. Gaston, Computational Materials Science **115**, 18-25 (2016).
[8] N. Moelans, B. Blanpain and P. Wollants, Physical Review B **88**, 054103(2013)
[9] P.V. Nerikar, K. Rudman, T.G. Desai, D. Byler, C. Unal, K.J. McClellan, S. Phillpot, S. Sinnott, P. Peralta, P. Uberuaga, and C. Stanek, Journal of the American Ceramic Society **94**,1893–1900 (2011).
[10] J.B. Ainscough, B.W. Oldfield, and J.O. Ware, Journal of Nuclear Materials **49** (2), 117-128 (1973).
[11] T. Heo, L. Zhang, Q. Du, and L.Q. Chen, Scripta Materialia **63**, 8-11 (2010).